01 Jul 2017

Homogenization of Plastic Deformation in Heterogeneous Lamella Structures

Rui Yuan

Irene J. Beyerlein

Caizhi Zhou
Missouri University of Science and Technology, zhouc@mst.edu

Recommended Citation

R. Yuan et al., "Homogenization of Plastic Deformation in Heterogeneous Lamella Structures," *Materials Research Letters*, vol. 5, no. 4, pp. 251-257, Taylor & Francis Ltd., Jul 2017.
The definitive version is available at https://doi.org/10.1080/21663831.2016.1255264

MATER. RES. LETT., 2016
http://dx.doi.org/10.1080/21663831.2016.1255264

MATERIALS RESEARCH LETTERS
Taylor & Francis
Taylor & Francis Group

Homogenization of plastic deformation in heterogeneous lamella structures

Rui Yuan[a], Irene J. Beyerlein[b] and Caizhi Zhou[a]

[a]Department of Materials Science and Engineering, Missouri University of Science and Technology, Rolla, MO, USA; [b]Materials Department, Department of Mechanical Engineering, University of California at Santa Barbara, Santa Barbara, CA, USA

ABSTRACT

It has been shown that unlike its constituent nanocrystalline (NC) phase, a heterogeneous lamella (HL) composite comprising NC and coarse-grain layers exhibits greatly improved ductility. To understand the origin of this enhancement, we present a 3D discrete dislocation, crystal plasticity finite element model to study the development of strains across this microstructure. Here we show that the HL structure homogenizes the plastic strains in the NC layer, weakening the effect of strain concentrations. These findings can provide valuable insight into the effects of material length scales on material instabilities, which is needed to design heterogeneous structures with superior properties.

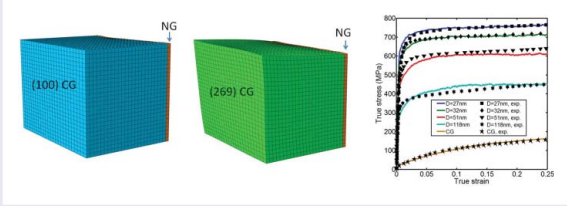

IMPACT STATEMENT

Our work reveals that the coarse-grain layer of a severely heterogeneous lamella composite homogenizes deformation in the nanocrystalline layer, resulting in the enhanced ductility for which this composite is renowned.

ARTICLE HISTORY
Received 7 October 2016
Accepted 26 October 2016

KEYWORDS
Dislocations; statistics; heterogeneous; strain gradients; instability

Introduction

The heterogeneous lamella (HL) metallic structures characterized with alternating lamellae of soft microcrystalline grains and hard nanocrystalline (NC) grains show great potential, not only because they simultaneously possess enhanced strength and considerable ductility, but also because the processes involved in fabricating them are cost-effective and can be scaled up for industrial production [1,2]. Recent pioneering work has shed some valuable insight into the fundamental principles that govern the desirable mechanical properties of HL structures. Ma et al. [3] fabricated specimens of Cu/bronze HL layers via high pressure torsion and found that the yield strength of the HL samples could be predicted by the rule of mixtures (ROM), yet the strain hardening rate was higher. Wu et al. [2] showed that HL Ti, synthesized via asymmetric rolling, exhibited both ultrafine-grained (UFG) strength and coarse-grained (CG) ductility. The high strength was attributed to an internal backstress generated at the lamellae interfaces via the constraint placed by the hard UFG layers on the soft micrograined layers. Since HL metallic structures have only been synthesized in recent years, the underlying mechanisms responsible for their unusual simultaneous high strength and good ductility are not well understood.

The various processing methods used to make HLs can induce different textures. Liu et al. [4,5] found that $\{100\}\ <011>$ was the dominant texture component, along with minor components $\{111\}\ <112>$ and $\{111\}\ <110>$ in nano-laminated nickel synthesized via surface mechanical grinding treatment (SMGT). In contrast, Fang et al. [6] reported a random crystallographic texture in the topmost layer of gradient nanograined Cu samples, also processed by SMGT. No publication to date has systematically studied the role of texture in the interactions between the dissimilar lamellae or the overall

CONTACT Caizhi Zhou zhouc@mst.edu Department of Materials Science and Engineering, Missouri University of Science and Technology, Rolla, MO 65409, USA

Supplemental data for this article can be accessed here. http://dx.doi.org/10.1080/21663831.2016.1255264

deformation behavior of the HL structures. To help accelerate and make manufacturing and design more cost-effective, modeling and simulation are ideal for studying such effects of texture, effects that cannot be easily or efficiently investigated experimentally. Therefore, a thorough investigation via a computational approach on the effect of crystallographic texture on the plastic deformation of HL ought to be insightful.

The primary objective of this work is to understand the fundamental principles giving rise to the observed enhanced strength and high ductility simultaneously possessed by HL metallic structures by developing a multiscale model bridging the gap between nanoscale dislocation activities and macroscopic deformation behavior in Cu samples with an HL CG/NC structure. The effect of crystallographic texture on the homogenization of plastic deformation is also investigated.

Methods

The crystal plasticity finite element (CPFE) method is a full-field numerical technique based on the solution of both stress equilibrium and strain compatibility [7]. It calculates spatially resolved mechanical fields, such as strain and stress, based on the imposed boundary conditions and grain–grain interactions. However, because most CPFE models either use phenomenological constitutive formulations to describe dislocation-induced property evolution, such as strain hardening, or treat dislocations in a homogenized and statistical manner, they are more applicable to CG than NC materials. As the dimensions of the crystals in NC materials become close to that of an individual dislocation, it would be more appropriate to model the discrete nature of dislocation slip.

To overcome this problem we developed a discrete-CPFE model that explicitly accounts for discrete dislocation slip events within a crystal plasticity framework [8,9]. In this model, it is assumed that a dislocation source forms at a grain boundary triple junction and is a dislocation line that is pinned at two adjacent grain boundaries. When the resolved shear stress (RSS) reaches or exceeds the critical RSS (CRSS) associated with a dislocation slip event, the dislocation source can be activated and slips across the grain interior, and is eventually becomes absorbed at the opposite grain boundary. Our discrete-CPFE model models not discrete dislocations but discrete slip events. Unlike conventional crystal plasticity models slip is scale dependent, and is modeled to occur in finite movements dictated by microstructural length scales. In this work, we use our discrete-CPFE model to simulate the mechanical behavior of the NC lamella of Cu within the HL structure. At the length scale of CG, dislocations glide in vast numbers and interact with each other during plastic deformation, accumulating forest dislocations that can impede further dislocation motion, leading to strain hardening. In this case, the dislocation density-based model is used to model the deformation in CG part. The details of our model are provided in the supplement.

The preceding constitutive formulations are written as a user-defined material (UMAT) subroutine and implemented into Abaqus computer-aided engineering. Symmetry boundary conditions are imposed on the simulation cell shown in Figure 1. Specifically, the $x-$, $y-$ and $z-$ surfaces are constrained from moving along the x, y and z directions, respectively, while the $x+$, $y+$ and $z+$ surfaces are free to move. Uniaxial tension is applied to the $x+$ surface along the x direction at a constant strain rate $\dot{\varepsilon} = 1 \times 10^{-4}\,\mathrm{s}^{-1}$. Each element is assigned a random crystallographic orientation, rendering the NC lamellae initially texture-free. In our calculations, compatibility and equilibrium are satisfied at the interface between the NC and CG lamellae. In addition, with CPFE, we can allow for heterogeneities in stress and strain from grain to grain, and account for grain neighborhood effects. However, in the present application to a NC material, since dislocations seldom accumulate inside the nano-grains, we assume that the greater heterogeneity develops between adjoining nano-grains and thus believe that one element representing one grain still can reasonably capture the plasticity of the NC part. Furthermore, for the calculations on NC lamella, the discrete-CPFE model is insensitive to the mesh size, as one element represents one grain. The CG part is modeled by one grain, which is meshed by 15,000 ($25 \times 25 \times 24$) elements. Our mesh-sensitivity tests indicate that the results are not sensitive to mesh size when the total number of elements becomes larger than 1000.

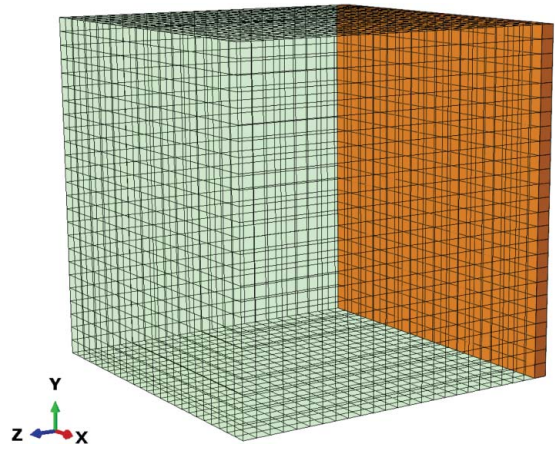

Figure 1. Mesh used in the HL structure comprising a NC layer (orange solid elements) and a single coarse grain (green empty elements).

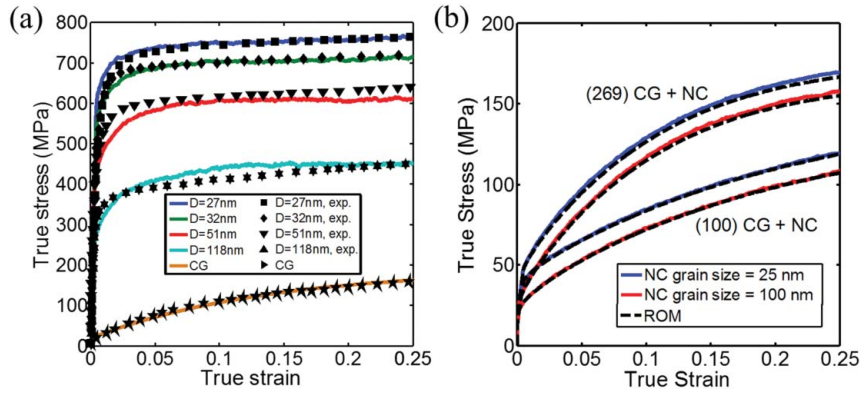

Figure 2. (a) Comparison between the experiment [10] and calculated stress-strain curves for texture-free NC cu at various grain sizes and for CG Cu. (b) Comparison of the stress-strain curves from CPFE and ROM calculations for different combinations of CG orientation and NC grain size.

Figure 2(a) compares the stress-strain curves of NC Cu at four different grain sizes calculated by the discrete-CPFE model and the stress-strain curves of CG Cu calculated by the homogenized strain hardening model with the experimental results from [10]. The stress-strain responses of both NC and CG Cu achieve good quantitative agreement with the experiment data in all aspects, such as yield strength, flow stress and strain hardening. We also observe that the pronounced grain-size effect in NC Cu is captured. The single set of parameters on which these calculations were made is listed in the supplementary materials and is adopted for all calculations throughout this study.

Comparison of results from CPFE and ROM calculations

The ROM is often used as a simple way of approximating the overall mechanical behavior of composites made of two or more materials, and the overall stress of the composite can be expressed as:

$$\sigma_{\mathrm{ROM}} = \sum V_i \sigma_i, \tag{1}$$

where σ_{ROM} is the overall stress of the laminated composite, σ_i and V_i are the stress and volume fraction of component i, respectively. As an ideal model, ROM does not take into consideration interactions among the constituent components; thus, it only holds true when such interactions are weak or non-existent [11]. In addition to inter-lamellar interaction, both grain size and crystallographic texture profoundly influence the mechanical behaviors of nanomaterials, such as yield strength, ductility, strain hardening, strain rate sensitivity and plastic anisotropy [12]. It is reasonable to speculate that grain size and crystallographic texture may also give rise to or influence interactions among the HL. Therefore, computational tests on HL-structured Cu samples consisting of an NC lamella at different grain sizes and CG lamellae with different textures were carried out. Specifically, grains in the NC lamella have a random initial crystallographic texture, i.e. they are texture-free. The CG textures are for initially (100)- and (269)-oriented grains, which indicate the single-slip and multiple-slip orientations, respectively.

Figure 2(b) compares the stress-strain curves from the CPFE model and with the ROM calculations. The results clearly demonstrate the grain-size-dependent strength characteristic of NC Cu, as the yield and flow stresses increase with decreasing NC grain size. At the same time, a significant texture effect is evident, as the samples with a (269) initial texture show higher yield and flow stresses than their respective (100)-textured counterparts.

In terms of strain hardening, samples with the same initial texture exhibit similar strain hardening behavior, while samples with a (269) texture strain harden more significantly than those with (100)-textured CG. In samples with a (100) initial texture, there are 8 equally favored slip systems for the activation of dislocation slip, and they are symmetrically distributed on each of the 4 {111} slip planes. As a consequence, grain rotation due to crystal slip under plastic deformation is suppressed due to balanced operations of the equally favored slip systems, giving rise to stable grain orientation of CG and lower strain hardening rate. Unbalanced crystal slip happens in samples with the (269)-oriented CG, resulting in CG grain rotation and higher strain hardening rates. Figure 3 compares equivalent plastic strain distribution for these two cases. We can see that the sample with the (269)-textured CG exhibits larger distortion than that with the (100)-textured CG.

Furthermore, the stress-strain curves from our CPFE calculations agree well with the ROM calculations. Besides our work, Ma et al. [3] also demonstrated that

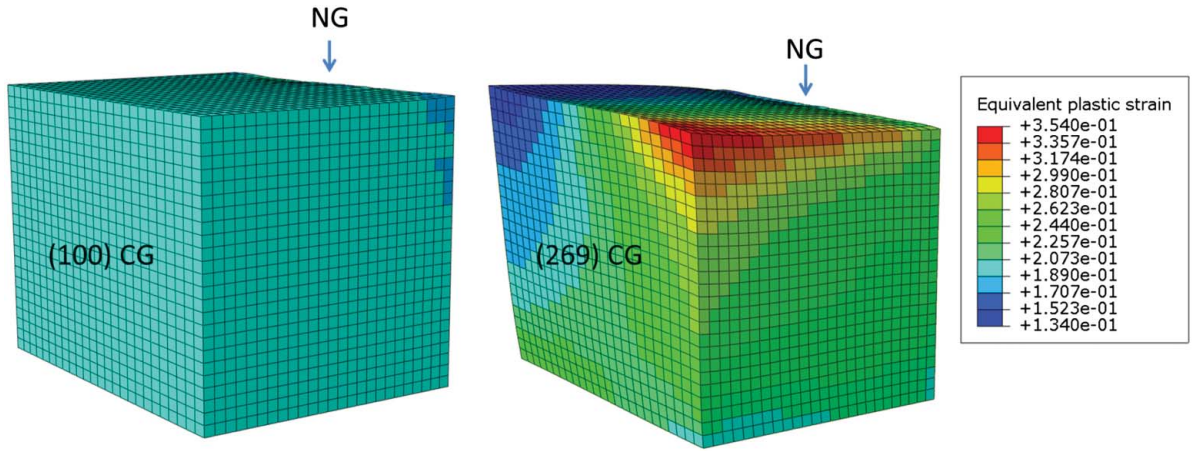

Figure 3. Comparison of equivalent plastic strain distribution in samples with (100)- and (269)-oriented CG after 20% deformation.

the uniaxial tensile strength of laminated samples can be predicted by ROM calculations. Moreover, the iso-strain condition that is the basis for the ROM best applies in the case where the loading direction is parallel to the CG/NG interface. As shown, reasonable agreement between ROM and CPFE calculations or experiment results is obtained.

Homogenization of strain distribution in NC lamella

While the discovery of extraordinary ductility in grain size-gradient (GSG) or HL structures has attracted much attention, its origin is not well understood. Some have postulated that it arises from enhanced strain hardening at the HL interfaces [1,2,13] while others have attributed it to a gradual shift in where plastic deformation initiates in the GSG structure [14].

The core of both viewpoints concerns how the HL structure modifies the distribution of strain and strain gradients within the NC and CG phases. The NC phase alone is not ductile with ductility typically declining as NC grain sizes decrease [12]. In NC metals, low ductility is primarily caused by void nucleation, and growth and their coalescence into cracks. Voids tend to form most often at grain boundary triple or quadruple junctions [15]. The process is statistical in nature in the sense that not all junctions form voids, but primarily at those where severe incompatibilities in plastic deformation among adjacent grains cause high strains and strains gradients to develop. Using the present model, we study the distribution of key plastic strain measures for different HL microstructures and compare them with the same distributions for the corresponding NC material.

One measure is the equivalent plastic strain $\varepsilon^{\mathrm{ep}}$, which is defined as:

$$\varepsilon^{\mathrm{ep}} = \sqrt{\frac{2}{3}(\boldsymbol{\varepsilon}^{\mathrm{p}} : \boldsymbol{\varepsilon}^{\mathrm{p}})}, \tag{2}$$

where ε^{p} is the plastic strain tensor. Strain localization is often induced by inhomogeneous plastic deformation.

Figure 4 shows the equivalent plastic strain distribution in the NC phase ($\sim$625 grains) of the HL Cu material at three levels of strain. Two CG orientations are shown with two different grain sizes, 100 and 25 nm, for the NC layer. In all cases, the variance in the plastic strains increases, signifying that the amount of statistically larger strain concentrated regions, the upper tails of the distribution, increases with strain. Thus the probability of shear localization amplifies with increasing strain, which is consistent with experiment results on NC metals [16,17].

The important result of the analysis in Figure 4 is that the NC layer within the HL structure has a more homogeneous strain distribution. This positive effect can be seen by direct comparison with the equivalent plastic strain distribution for single-phase NC Cu with the same grain sizes. For all NC grain sizes, the inhomogeneity in plastic strain in the HL composite is less than that for single-phase NC. The HL composite has a narrower and hence more homogeneous equivalent plastic strain distribution. Compared to single-phase NC Cu, the HL Cu is less likely to experience strain localization at the same strain level. The analysis also suggests an important texture effect. The distribution in plastic strain is less dispersed for the HL composite with the (100)-oriented grain than the (269) one. The latter is well oriented for multi-slip, whereas the latter planar slip. Hence the homogenization effect arising from the HL composite can be further

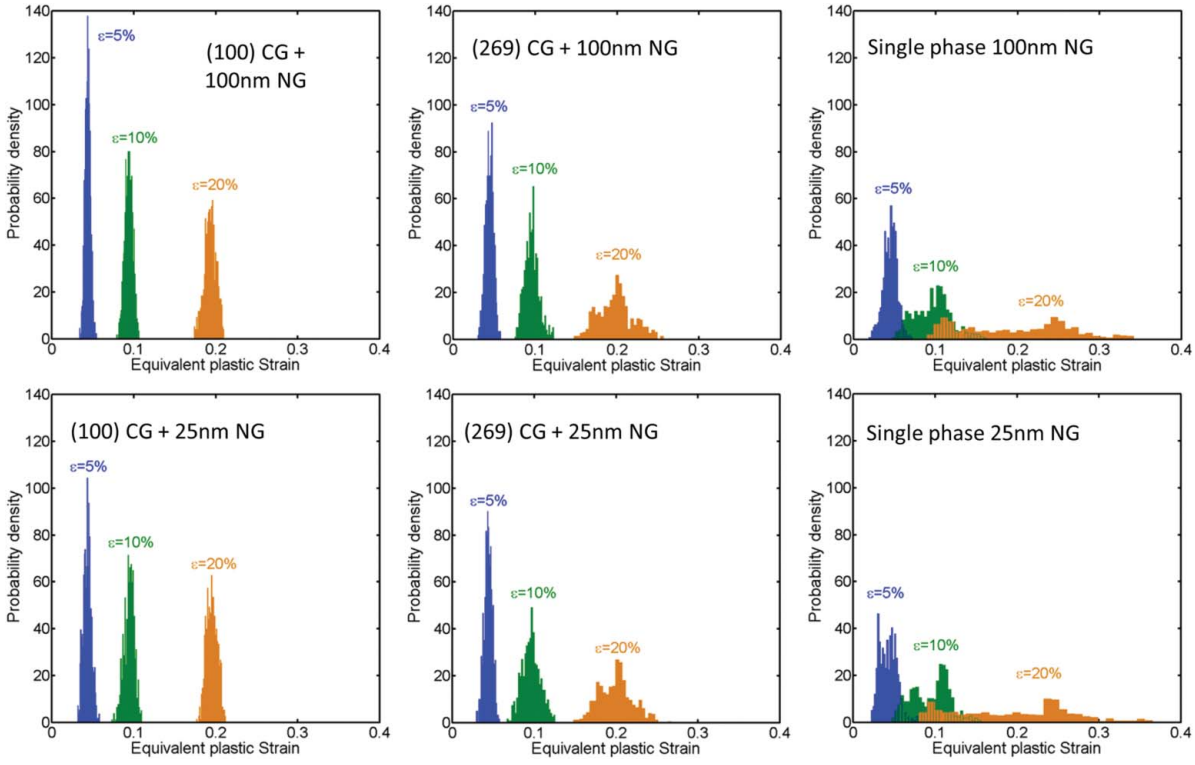

Figure 4. Equivalent plastic strain distribution in NC lamella in HL Cu samples with 25 and 100 nm NC grain sizes and (100) and (269) CG textures, along with the distribution in a stand-alone layer of pure NC Cu. In all cases, the variance in the plastic strains increases, signifying that the amount of statistically larger strain concentrated regions, the upper tails of the distribution, increases with strain.

improved when the CG phase undergoes homogeneous deformation.

To elucidate reorientation gradients, we choose to calculate the fields of reorientation angle in the HL structures, where reorientation angle is defined as the difference in orientation of a grain before and after deformation (see details in the supplement). In recent work, Ardeljan et al. [15] showed via CPFE modeling that large differences in reorientation propensity at grain triple or quadruple junctions are strongly correlated with the development of large strain concentrations and strain localization. Neighboring grains with dissimilar reorientation propensities reorient in different directions creating even greater disparity with straining. Consequently at the junctions where they meet, large strain levels and strain incompatibilities develop that directly correlate to the onset of shear banding. Hence analyzing inhomogeneities in grain reorientation propensities can reveal the tendency for strain localization and shear banding.

To best elucidate the variance in the grain reorientation propensities across the NC layer, we present the reorientation angle distribution for the same cases as in Figure 4 in a Weibull probability graph [18]. The calculation procedures used to extract the reorientation angle are provided in the supplement. Figure 5 shows the Weibull probability plots of the reorientation angle distribution in the HL Cu samples with (100) CG texture compared with that in single-phase NC Cu, respectively. Each distribution consists of 625 reorientation angles arranged in ascending order. The abscissa represents $\ln(\alpha)$ and the ordinate $\ln(-\ln(1-P_f))$, where P_f is the probability and is calculated as:

$$P_f = \frac{r - 0.5}{N}, \tag{3}$$

where r is the numerical rank of each reorientation angle in the distribution (the reorientation angles were ranked in ascending order by radians) and N is the sample size. The slope of a line represents the Weibull modulus and is a measure of the variability of the distribution. From Figure 5, we clearly see that the Cu with HL structure consistently shows a higher Weibull modulus than single-phased pure NC Cu for all grain sizes and strain levels, indicating that grain reorientation propensities in the NC lamella in HL Cu are lower in variability and more uniform than those in pure NC Cu. Furthermore, such a difference becomes more pronounced as the strain increases from 5% to 20%. An analysis of the variability of NC grain reorientation propensities in HL Cu samples with (269) CG texture demonstrates the same trend. The higher degree of uniformity in terms of grain reorientation propensities in HL-structured Cu samples indicates

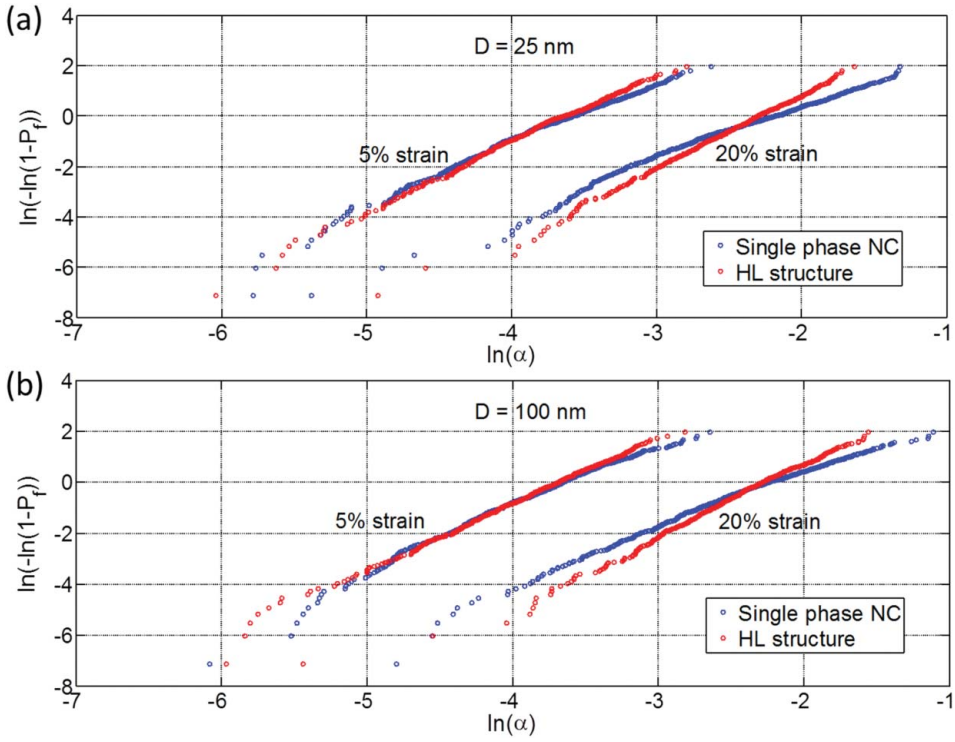

Figure 5. Weibull probability graphs of the reorientation angle distribution in HL Cu samples with (100) texture CG and pure NC Cu samples at 5% and 20% strain, respectively. The NC grain sizes are (a) 25 and (c) 100 nm, respectively. The Cu with HL structure consistently shows a higher Weibull modulus than single-phased pure NC Cu, indicating that grain reorientation propensities in the NC lamella in HL Cu are lower in variability and more uniform than those in pure NC Cu.

that strain concentration is less likely to develop, hence shear bands are less likely to form as a result of such strain localization in these samples.

The results from the analysis of the reorientation angle distribution indicate that the CG lamellae in the HL-structured composite homogenizes the grain reorientation tendencies of NGs, leading to less areas of high strain localization and a lower likelihood for shear band formation. This is also consistent with the foregoing equivalent plastic strain analysis, which suggests that the CG lamellae homogenize the plastic strains within the NC layer. The consequence is an enhancement in the ductility of the HL-structured composite, which significantly also exhibits high strength.

Conclusions

In this work, we employ a 3D discrete-CPFE model to study the deformation of HL metallic composite structures and understand the fundamental principles governing their high strength and good ductility. The model HL composite consists of alternating NC and CG lamellae, which exhibit a two to three order of magnitude difference in grain size. The calculation distinctively captures the coupled effect of grain-size-dependent strength induced by the NC lamella and the texture effect in the CG lamellae. Based on the analysis of the distributions of the equivalent plastic strain and reorientation angles within the NC lamella, we found that the heterogeneity of strain concentration, which induces the shear localization in the nanograin part, has been reduced by the uniform deformation of coarse-grain lamella. Coarse grains well oriented for multi-slip further homogenize the plastic deformation in the NC lamella, thereby potentially increasing the ductility of the HL structure. These findings can provide valuable insight into improving nanomaterial processing techniques, and have implications for the design of gradient or heterogeneous structures with superior properties.

Disclosure statement

No potential conflict of interest was reported by the authors.

Funding

This work was supported by the grants from The University of Missouri Research Board. C.Z. is also grateful for the partial support provided by Materials Research Center at Missouri University of Science and Technology. I.J.B. gratefully acknowledges an NSF STEM ADVANCE scholarship from the University of New Hampshire.

References

[1] Wu X, Jiang P, Chen L, et al. Extraordinary strain hardening by gradient structure. Proc Natl Acad Sci. 2014;111:7197–7201.

[2] Wu X, Yang M, Yuan F, et al. Heterogeneous lamella structure unites ultrafine-grain strength with coarse-grain ductility. Proc Natl Acad Sci. 2015;112:14501–14505.

[3] Ma XL, Huang CX, Xu WZ, et al. Strain hardening and ductility in a coarse-grain/nanostructure laminate material. Scr Mater. 2015;103:57–60.

[4] Liu XC, Zhang HW, Lu K. Formation of nano-laminated structure in nickel by means of surface mechanical grinding treatment. Acta Mater. 2015;96:24–36.

[5] Liu XC, Zhang HW, Lu K. Strain-induced ultrahard and ultrastable nanolaminated structure in nickel. Science. 2013;342:337–340.

[6] Fang TH, Li WL, Tao NR, et al. Revealing extraordinary intrinsic tensile plasticity in gradient nano-grained copper. Science. 2011;331:1587–1590.

[7] Roters F, Eisenlohr P, Hantcherli L, et al. Overview of constitutive laws, kinematics, homogenization and multiscale methods in crystal plasticity finite-element modeling: theory, experiments, applications. Acta Mater. 2010;58:1152–1211.

[8] Yuan R, Beyerlein IJ, Zhou C. Emergence of grain-size effects in nanocrystalline metals from statistical activation of discrete dislocation sources. Acta Mater. 2015;90:169–181.

[9] Yuan R, Beyerlein IJ, Zhou C. Statistical dislocation activation from grain boundaries and its role in the plastic anisotropy of nanotwinned copper. Acta Mater. 2016;110:8–18.

[10] Khan AS, Farrokh B, Takacs L. Compressive properties of Cu with different grain sizes: sub-micron to nanometer realm. J Mater Sci. 2008;43:3305–3313.

[11] Wu XL, Jiang P, Chen L, et al. Synergetic strengthening by gradient structure. Mater Res Lett. 2014;2:185–191.

[12] Meyers MA, Mishra A, Benson DJ. Mechanical properties of nanocrystalline materials. Prog Mater Sci. 2006;51:427–556.

[13] Yang M, Pan Y, Yuan F, et al. Back stress strengthening and strain hardening in gradient structure. Mater Res Lett. 2016:1–7.

[14] Lu K. Making strong nanomaterials ductile with gradients. Science. 2014;345:1455–1456.

[15] Ardeljan M, Knezevic M, Nizolek T, et al. A study of microstructure-driven strain localizations in two-phase polycrystalline HCP/BCC composites using a multi-scale model. Int J Plasticity. 2015;74:35–57.

[16] Witney AB, Sanders PG, Weertman JR, et al. Fatigue of nanocrystalline copper. Scripta Metall Mater. 1995;33:2025–2030.

[17] Wei Q, Jia D, Ramesh KT, Ma E. Evolution and microstructure of shear bands in nanostructured Fe. Appl Phy Lett. 2002;81:1240–1242.

[18] Landis CM, Beyerlein IJ, McMeeking RM. Micromechanical simulation of the failure of fiber reinforced composites. J Mech Phys Solids. 2000;48:621–648.